JCTC Journal of Chemical Theory and Computation

Molecular Orbital-Averaged Fukui Function for the Reactivity Description of Alkaline Earth Metal Oxide Clusters

Nick Sablon,* Frank De Proft, and Paul Geerlings

Vrije Universiteit Brussel, Eenheid Algemene Chemie, Pleinlaan 2, B-1050 Brussel, Belgium

Received January 16, 2009

Abstract: This paper concerns the accurate description of the surface oxygen reactivity for the alkaline earth metal oxides using local DFT-based reactivity indices. The cumbersome periodic boundary conditions calculations, typically required to probe the reactivity of such systems, are avoided by the construction of a reliable cluster model. The standard Fukui function concept of conceptual DFT is generalized to include the contribution from not only the HOMO and the LUMO but also from other chemically relevant orbitals. Results prove that this approach is a valuable and straightforward alternative to the reactivity calculation of extended systems.

1. Introduction

In general, chemical reactions are driven by a change in the reagents' number of electrons and a rearrangement of their nuclei. Conceptual density functional theory[1−4] (DFT) exploits this observation to define various reactivity descriptors for the interpretation of chemical reactions. First and higher order (functional) derivatives of the electronic energy with respect to the electron number N or the external potential $v(\mathbf{r})$, which is just the electron−nuclear potential for isolated atoms and molecules, are identified with quantities of chemical relevance. Concepts such as the electronic chemical potential or the electronegativity,[5] the chemical hardness and softness,[6] the Fukui function,[7,8] etc., could sharply be defined in this context and have been applied in many studies to interpret both theoretical and experimental data.[3]

Nowadays the practical computation of these reactivity descriptors usually occurs in a Kohn−Sham (KS) DFT scheme,[9] in which the introduction of the so-called Kohn−Sham molecular orbitals (KS MOs) is key in the efficient application of the variational procedure for the electron density.[10] It turns out that the highest occupied and lowest unoccupied molecular orbitals (HOMO and LUMO) are the primary contributors to the characteristics of the various DFT-based concepts.[11−13] In this perspective, conceptual DFT can to some extent be seen as a generalization of the frontier molecular orbital (FMO) theory taking care of orbital relaxation effects and broadening the range of concepts.

Although it is clear that the HOMO and LUMO play a decisive role in the description of molecules with well-separated MO energy levels, is it also the case when these energy levels are closely spaced and an intermediate situation between the discrete MO levels and the continuous bands occurs? This problem will be addressed in the current paper. We will show that the prominent role of the HOMO and the LUMO should in certain cases be reassigned to and distributed among one or more other orbitals which leads to the introduction of the concept of the MO-averaged Fukui function.

This approach, which can be considered as an approximation to the local density of states-based Fukui function for extended systems, will be tested in a study of the (100) surface reactivity of the alkaline earth metal oxides MgO, CaO, SrO, and BaO. These systems are of particular interest because of their catalytic characteristics and their use in various technological applications. They are for example used in the oxidation process of methane[14] and for the destructive adsorption of chlorinated hydrocarbons.[15] Calculation of the reactivity of the electron rich surface oxygen centers is the main goal of this paper since these atoms are highly reactive toward electophilic attacks[16−18] and could be considered as superbasic sites.[19] The central idea is to use the well-established conceptual DFT framework for mol-

* Author to whom correspondence should be addressed. E-mail: nsablon@vub.ac.be.

10.1021/ct9000312 CCC: $40.75
Published on Web 04/10/2009

ecules in this study in order to avoid the cumbersome infinite system calculations. Even though a simple diatomic gas-phase system could give some reactivity indications, the surface characteristics are inaccessible by this kind of simplified model system. It has, for example, been observed that reactivity trends for bulk and surface atoms of the same systems can be different.[20] This is the reason why we have opted for the use of an embedded cluster approach to construct a rigorous surface model.

The paper is organized as follows. In Section 2 the necessary elements of conceptual DFT are summarized and the MO-averaged Fukui function concept is introduced. Section 3 briefly reviews some of the approaches to construct reliable cluster models, explains the model used, and analyzes the properties of the alkaline earth oxide clusters. Methodological details and the surface reactivity results are discussed in the fourth section. The final conclusions are given in Section 5.

2. Theoretical Background

2.1. The Fukui Function. As this paper primarily concerns the local description of chemical reactivity, global reactivity or stability indicators will not be discussed in detail here. We will, however, give some theoretical information on the Fukui function $f(\mathbf{r})$, which is the concept of interest in a local description of reactions that are driven by the so-called soft−soft interactions. Parr and Yang[7] defined this concept as the second derivative of the electronic energy E with respect to the number of electrons N and the external potential $v(\mathbf{r})$:

$$f(\mathbf{r}) = \frac{\partial^2 E}{\delta v(\mathbf{r}) \partial N} \tag{1}$$

Using the following relations for the electron density $\rho(\mathbf{r})$ and the electronic chemical potential μ,

$$\rho(\mathbf{r}) = \left(\frac{\delta E}{\delta v(\mathbf{r})}\right)_N \tag{2}$$

$$\mu = \left(\frac{\partial E}{\partial N}\right)_{v(\mathbf{r})} \tag{3}$$

two equivalent expressions for the Fukui function can be found:

$$f(\mathbf{r}) = \left(\frac{\partial \rho(\mathbf{r})}{\partial N}\right)_{v(\mathbf{r})} = \left(\frac{\delta \mu}{\delta v(\mathbf{r})}\right)_N \tag{4}$$

The derivatives with respect to N in eqs 1, 3, and 4 imply that one must introduce a noninteger number of electrons. This was done by Perdew et al.[21] in a zero temperature grand canonical ensemble framework, which showed that for exact solutions to the Schrödinger equation the electronic energy, like the electron density evaluated at a certain point in space, as a function of N is made up of a series of straight line segments that intersect at integer electron number.[22,23] These derivatives should consequently be replaced by right- and left-hand side derivatives at the integer electron number. Within an exact theory the chemical potentials and the Fukui functions from above, μ^+ and $f^+(\mathbf{r})$, and from below, μ^- and $f^-(\mathbf{r})$, are thus given by

$$\mu_K^+ = \left(\frac{\partial E}{\partial N}\right)_{v(\mathbf{r})}^+ \Bigg|_{N=K} = E_{K+1} - E_K \tag{5}$$

$$\mu_K^- = \left(\frac{\partial E}{\partial N}\right)_{v(\mathbf{r})}^- \Bigg|_{N=K} = E_K - E_{K-1} \tag{6}$$

$$f_K^+(\mathbf{r}) = \left(\frac{\partial \rho(\mathbf{r})}{\partial N}\right)_{v(\mathbf{r})}^+ \Bigg|_{N=K} = \rho_{K+1}(\mathbf{r}) - \rho_K(\mathbf{r}) \tag{7}$$

$$f_K^-(\mathbf{r}) = \left(\frac{\partial \rho(\mathbf{r})}{\partial N}\right)_{v(\mathbf{r})}^- \Bigg|_{N=K} = \rho_K(\mathbf{r}) - \rho_{K-1}(\mathbf{r}) \tag{8}$$

at an integer number of electrons K. Equation 7 allows the interpretation of $f_K^+(\mathbf{r})$ to describe the propensity of a molecular site to undergo nucleophilic attacks, while eq 8 shows that $f_K^-(\mathbf{r})$ is able to describe the reactivity toward electrophilic attacks.

These finite difference formulas (eqs 5−8) are however not exact anymore when practical DFT calculations with approximate exchange-correlation functionals are carried out.[8] The correct behavior of the Fukui functions $f_K^{\pm}(\mathbf{r})$ within such an approximate theory can thus only be obtained through a direct evaluation of the derivative in eq 1. Based on the fact that DFT calculations are rooted in the KS approach and using Janak's theorem,[24]

$$\left(\frac{\partial E}{\partial n_i}\right) = \varepsilon_i \tag{9}$$

where n_i and ε_i denote the occupation number and the energy of the ith MO, the derivatives of E with respect to N are given by the KS HOMO and LUMO energies,

$$\left(\frac{\partial E}{\partial N}\right)_{v(\mathbf{r})}^+ = \varepsilon_{\mathrm{LUMO}} \tag{10}$$

$$\left(\frac{\partial E}{\partial N}\right)_{v(\mathbf{r})}^- = \varepsilon_{\mathrm{HOMO}} \tag{11}$$

which implies the following expressions for the Fukui functions:

$$f^+(\mathbf{r}) = \left(\frac{\delta \varepsilon_{\mathrm{LUMO}}}{\delta v(\mathbf{r})}\right)_N \tag{12}$$

$$f^-(\mathbf{r}) = \left(\frac{\delta \varepsilon_{\mathrm{HOMO}}}{\delta v(\mathbf{r})}\right)_N \tag{13}$$

(Equations 10 and 11 also hold for an exact KS theory if $\varepsilon_{\mathrm{LUMO}}$ and $\varepsilon_{\mathrm{HOMO}}$ are replaced by $\varepsilon_{\mathrm{LUMO}}^+$ and $\varepsilon_{\mathrm{LUMO}}^-$, which are the frontier orbital energies associated with the exact exchange-correlation potential from above $v_{xc}^+(\mathbf{r})$ and from below $v_{xc}^-(\mathbf{r})$, respectively.[21,22,25] The difference between the two exchange-correlation potentials disappears for local approximations to the exchange-correlation functional (LDA and GGA) so that eqs 10 and 11 can be used.)

So, the Fukui functions can readily be obtained by evaluation of these functional derivatives, for which a methodology is explained in Section 4.

Equations 12 and 13 are clear examples of the importance of the HOMO and the LUMO in conceptual DFT. Other exact relations for the Fukui functions, obtained by Yang et al., are a further illustration:[1,7,11,26]

$$f^{+}(\mathbf{r}) = \sum_{s}\left\{|\psi_{\mathrm{LUMO}}(\mathbf{x})|^2 + \sum_{i=1}^{N}\left(\frac{\partial|\psi_i(\mathbf{x})|^2}{\partial N}\right)^{+}_{\nu(\mathbf{r})}\right\} \quad (14)$$

$$f^{-}(\mathbf{r}) = \sum_{s}\left\{|\psi_{\mathrm{HOMO}}(\mathbf{x})|^2 + \sum_{i=1}^{N}\left(\frac{\partial|\psi_i(\mathbf{x})|^2}{\partial N}\right)^{-}_{\nu(\mathbf{r})}\right\} \quad (15)$$

with $\psi_i(\mathbf{x})$ the KS MOs, depending on a position coordinate $\mathbf{r}$ and a spin coordinate s. The main contribution to the Fukui functions can be ascribed to the probability density of the frontier MOs. Relaxation effects of all the orbitals are, nonetheless, taken into account, which is an improvement to the FMO theory.

2.2. The MO-Averaged Fukui Function. The dominant role the HOMO and the LUMO play in the description of chemical reactivity can be traced back to the underlying assumption that when electron transfer occurs during the chemical reaction the removal or addition of electrons take place in these orbitals. Although this has been shown to be a valid approach in very many cases,[3] for systems presenting a number of closely lying frontier orbitals this might pose serious problems. In the past this has, for example, led to approaches that consider the HOMO-1 orbital in order to probe the reactivity toward electrophiles.[27] The HOMO and LUMO are also generally localized on the most reactive site; even so, one can be interested in a reactivity description of another molecular part, where these orbitals are not necessarily well represented, as it could be more prone to reaction due to steric effects or when a comparison with an analogous site in another molecule is the aim. We recently observed for example that the directing effect of substituents in the electrophilic aromatic substitution reactions of simple monosubstituted benzenes could not always be recovered by the information contained in the HOMO in case of it predominantly being located on the substituent and not on the aromatic ring.[27] For larger systems having a number of closely spaced MO energy levels (which could be seen as a precursor of the band structure in infinite systems), it is irrelevant to pick just one orbital out for the reactivity description while ignoring the others.

These observations suggest that the classical Fukui function concept as introduced above should be extended in certain cases. Other orbitals should be able to enter eqs 12−15 on the same footing as the frontier orbitals. We propose two criteria to rigorously determine the appropriate orbitals and their contribution to the reactivity description, which will lead to the definition of the MO-averaged Fukui function ($\tilde{f}^{+}(\mathbf{r})$ or $\tilde{f}^{-}(\mathbf{r})$) concept.

The first one is an energetic criterion. It is clear that only orbitals which have the energetic potential to exert a substantial chemical influence (which have an energy comparable to the HOMO or LUMO energy) should be considered. (It is interesting to note that, in the case where the orbital energy spacing is very small, energetic responses induced by perturbations in the external potential are likely to exceed this spacing so that the Fukui functions are only strictly defined within a degenerate perturbation theoretical framework. The averaging proposed in eqs 16 and 17 is, however, a more straightforward approach which includes the responses of the necessary orbitals for a reliable reactivity description. This observation was brought up by an anonymous referee, who the authors wish to acknowledge.) A close inspection of the MO energy levels is thus required in order to select the relevant orbitals. A spatial criterion, on the other hand, demanding that the included orbitals are particularly situated on the reactive site of interest is indispensable when an intermolecular reactivity scale of a specific molecular site is desired. This can be assured by weighting the various orbital contributions with a factor that is proportional to the orbitals' probability density at this site. The MO-averaged Fukui functions summarize all these requirements and are defined as

$$\tilde{f}^{+}(\mathbf{r}) = \sum_{i} w_i f_i^{+}(\mathbf{r}) \quad (16)$$

$$\tilde{f}^{-}(\mathbf{r}) = \sum_{i} w_i f_i^{-}(\mathbf{r}) \quad (17)$$

where w_i are the aforementioned weighting factors and where the index i in eq 16 runs over all the unoccupied MOs satisfying the energetic criterion, while it considers the occupied ones in eq 17. It should be stressed that the inclusion of the weighting factors is not to be done if one wants to discern the various reactive regions within a molecule and compare their relative importance. $f_i^{+}(\mathbf{r})$ and $f_i^{-}(\mathbf{r})$ denote alternative Fukui functions which are analogous to the ones in eqs 12 to 15, apart from the fact that the LUMO or the HOMO are exchanged for the ith unoccupied or occupied MO respectively, and reflect the reactive behavior of this orbital with respect to a nucleophilic or electrophilic attack. The introduction of these alternative Fukui functions is in total agreement with Janak's theorem if one assumes that the electron addition or withdrawal indeed occurs in these orbitals.

An explicit expression for the calculation of the weighting factors w_i will be presented in Section 4, where the dramatic improvement of the reactivity description by application of eq 17 will be extensively discussed as well. But before this can be done, we will elaborate on the kind of systems to be analyzed and more specifically on the choice of the cluster model for the alkaline earth oxides and on the electronic structure of the reactive site of interest.

3. Cluster Models and Analysis of the Alkaline Earth Oxide Clusters

The modeling of infinite systems as solids and solid surfaces by finite clusters has been discussed in a vast amount of papers. Often metal oxides are concerned because of the interest in their reactivity properties, which include adsorption characteristics, crystal defects, electronic structure, and catalytic activity. Many approaches have been proposed to construct appropriate clusters that accurately simulate the genuine solid state and to improve their performance. The

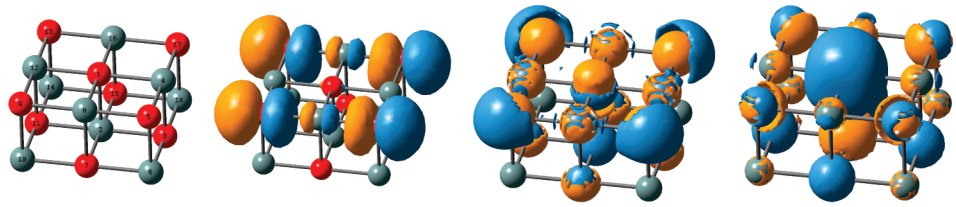

Figure 1. Sr_9O_9 cluster. (a) Representation of the cut-out cluster with atom 1 at the center as the surface oxygen of interest. (b) Isosurface of the HOMO with an isovalue of 0.02 au. (c) Isosurface of the Fukui function from below $f^-(\mathbf{r})$, calculated with eq 13, with an isovalue of 0.002 au. (d) Isosurface of the MO-averaged Fukui function from below $\tilde{f}^-(\mathbf{r})$, calculated with eq 17, with an isovalue of 0.002 au.

first paragraph of this section briefly reviews the most common ones in order to justify our model chosen. A discussion of the whole panoply of available methods lies beyond the scope of this paper. The second paragraph applies our model of choice to the calculation of MgO, CaO, SrO, and BaO and analyses their cluster properties.

3.1. Cluster Models. In the case of metal oxides, a subdivision can be made between the bare, embedded, and saturated cluster models.[28] A bare cluster only consists of a piece of the bulk structure, and its relevance is often strongly dependent on a fortuitously good choice of geometry and size.[29] It is clear that an improved description results from incorporating the effect of the rest of the bulk, which is not explicitly taken into account in the quantum chemical calculations. For ionic solids, as the alkaline earth oxides, an embedding procedure which mimics the potential created by the rest of the bulk by surrounding the cluster with an array of point charges is the most common and effective approach.[30,31]

As the embedding potential is a correction to the bare cluster for the neglected bulk effects (i.e., the electrostatic or Madelung potential and boundary interactions), the cut-out should rigorously be done so as to represent the bulk situation as accurately as possible. Lü et al.[31,32] defined three practical rules that ensure an easy and good choice. These are the stoichiometry, neutrality, and coordination principles. The use of a stoichiometric cluster seems to improve results because spurious energy levels coming from excess atoms are avoided.[33] Moreover, the neutrality condition will then automatically be fulfilled. In order to be in line with the coordination principle, a cluster should contain the strongest bonds within it.

Various embedding schemes have been developed. As indicated above, methods based on cluster enclosure in an array of point charges are prevalent, though other possibilities such as the hybrid quantum mechanical/molecular mechanical (QM/MM) treatment exist.[34] The easiest approach is to place point charges at the ideal lattice positions and assign them values equaling the ionic charges of the crystal. This model can be refined by replacing the positive charges closest to the cluster by pseudopotentials.[35] An overpolarization of the neighboring cluster anions is thus avoided, which improves the description of the boundary interactions. A typical problem of these models is the slow or even absence of convergence as the array is expanded.

Stefanovich and Truong[36] stressed the need of well-chosen and optimized point charge arrays. The disadvantage of many methods[37−41] is that the optimal embedding charges are defined as the ones that reproduce a reference electrostatic potential which is assumed to be originating from a lattice consisting of ions bearing the formal ionic charges. This cannot be entirely justified, as all chemical bonds to some extent have a covalent component.

This obstacle can be overcome by optimizing the surrounding point charges in a manner that experimental data of the bulk material is reproduced by the cluster model. Xu et al.[31] varied the charges, placed at the genuine lattice positions, from 0.0 to ± 2.0 au in a study of CO adsorption on a MgO surface and determined an ideal value on the basis of the correspondence of calculated electronic and geometric properties with experimental ones. They observed indeed that electronic characteristics were strongly dependent on the value of the embedding point charges and that the nominal value of ±2.0 au overestimates the crystal potential. Their results underscore the need to draw a clear distinction between the formal charges of the ions constituting the real crystal and the embedding charges which best represent the rest of the infinite solid for a specific cluster.

We based our cluster model on a recent study of Kadossov et al.[29] The embedding point charges are located at the ideal lattice positions (the negative ones at the oxygen anion positions and the positive ones at the cationic sites), a choice that should lead to the best results.[40] Their values are determined by performing geometry optimizations and requiring a correspondence of the calculated lattice parameter with the experimental one. It is shown in ref 29 that this is a sufficient demand to ensure electronic properties being decently described.

3.2. Analysis of the Alkaline Earth Oxide Clusters. Before determination of the optimal values of the surrounding point charges, a well cut-out cluster needs to be constructed. As metal oxides are generally ionic species, their electronic structure has a rather localized nature, which implies that converged results with respect to cluster size are readily obtained with medium sized clusters.[31,42] We have therefore decided to use Me_9O_9 clusters (Me = Mg, Ca, Sr or Ba) with the atoms placed at the experimental rock salt structure positions in a 3 × 3 × 2 geometry, as can be seen in Figure 1a for the Sr_9O_9 case. Because we are focused on the reactive behavior of the surface O-atoms, the central oxygen in the upper layer constitutes the reactive site in this study. It is the only atom which is completely surrounded by quantum atoms, except for the surface side, of course, and consequently suffers the least from boundary effects. It is important

Table 1. Absolute Value of the Optimal Point Charges, q, Yielding the Experimental Lattice Parameter a_{exp} upon Geometry Optimization

system	q, au	a_{exp}, Å
MgO	0.427	4.21
CaO	0.516	4.81
SrO	0.444	5.11
BaO	0.510	5.52

to point out that the cluster matches the correct local C_{4v} symmetry of the reactive site which is essential for a realistic model.

The three principles mentioned in paragraph 3.1 are fulfilled. The stoichiometry and neutrality requirements are clearly satisfied, as is the coordination condition since the chosen geometry is the arrangement containing the most bonds.

The clusters are embedded in four layers of point charges at each side, apart from the surface one, which results in an $11 \times 11 \times 6$ point charge array at the genuine lattice positions. The authors of ref 29 for example analyzed the effect of larger embedding arrays and concluded that no significant improvement could be observed. Geometry optimizations for the clusters are performed for charge values varying form 0.0 to ± 2.0 au, and the ideal charges are identified as the ones giving rise to the experimental lattice parameters. We used the eigenvalue-following algorithm[43] as optimization technique with the lattice parameter as the only variable. All bonding angles were fixed at 90° so that the undistorted rock salt structure was assured. DFT calculations were done with the B3LYP approximation to the exchange-correlation functional.[44] The 6-311++G* basis set[45] was used for the O atoms, whereas we opted for the Stuttgard/Dresden pseudopotentials and corresponding basis sets for the metal atoms.[46] One should be cautious when selecting the number of core electrons to be replaced by a pseudopotential. As the metal atoms are in their cationic form, it is important to explicitly treat not only the two electrons from the outer shell, which are in fact partially removed by the surrounding oxygens, but also those from the lower shell. We therefore used the MWB10 pseudopotential and basis set for Ca, the MWB28 for Sr, and the MWB46 for Ba. For Mg, no pseudopotential satisfies the requirement and so the all-electron 6-311++G* basis set was used. All calculations were performed with the Gaussian 03 program.[47]

Table 1 summarizes the results of the point charge optimization. It seems that the embedding charges have ideal values of around $\pm$ 0.5 au, largely deviating from the formal charge values of ± 2.0 au. This clearly indicates that care should be taken when using formal charges in the construction of an embedding scheme, even for highly ionic systems. Incidentally, a formal charge embedding in our cluster model gives rise to an overestimation of the lattice parameter by roughly 50%, which indicates the very poor representation of the crystal potential with such an approach.

We conclude this section with a few notes on the electronic structure of the clusters in order to show the need for the MO-averaged Fukui function concept in the local reactivity description. As we want to investigate a reactivity trend of the surface oxygen anions, which are prone to electrophilic attacks, we only consider the (MO-averaged) Fukui function from below. The standard Fukui function $f^-(\mathbf{r})$ (eqs 13 and 15) gets its main contribution from the HOMO, which is given in Figure 1b for Sr_9O_9 and which has analogous characteristics in the other cases. The HOMO is, however, mainly located on the cluster edges and shows almost no density at the central surface oxygen. $f^-(\mathbf{r})$ will consequently not provide any significant reactivity information on the reactive site of interest but rather probes artificial edge effects. An analysis of the clusters' electronic structure holds the clue how $\tilde{f}^-(\mathbf{r})$ solves the problem.

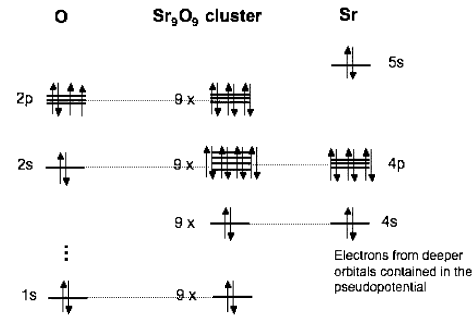

Figure 2. Schematic representation of the MO diagram of the Sr_9O_9 cluster.

Figure 2 gives a schematic representation of the MO diagram for the Sr_9O_9 cluster. Globally, the lowest 9 MOs are nonbonding orbitals with O-1s character; the next 9 MOs are nonbonding as well but now composed of the Sr-4s atomic orbitals. Then 36 MOs are found which are important contributors to the bonding of the cluster, as the O-2s and Sr-4p orbitals are mixed, whereas the final 27 occupied MOs are just located on the oxygens and are combinations of the O-2p atomic orbitals. The ionic character of the system manifests itself in the fact that the Sr-5s electrons move to the free O-2p places upon bonding. Most importantly, the 27 highest occupied MOs are linear combinations of the 2p atomic orbitals from the various O-atoms and thus all provide important contributions to the description of their reactivity and should be considered in the calculation of $\tilde{f}^-(\mathbf{r})$. Analogous conclusions can be drawn for the other systems. The calculation of the weighting factors w_i (eq 17) for these orbitals will be presented in the next section. The energetic criterion for MOs to enter the $\tilde{f}^-(\mathbf{r})$ expression is satisfied as the 27 highest orbitals are closely spaced (typically by 10^{-1} eV) and clearly energetically distinguishable from the others (with a typical gap of 10 eV).

4. Methodological Details and Practical Results

4.1. Calculation of the MO-Averaged Fukui Function. As mentioned in the theoretical section, the Fukui functions $f_i^-(\mathbf{r})$ needed in eq 17 are calculated as functional derivatives of the ith orbital energy ε_i with respect to $v(\mathbf{r})$:

$$f_i^-(\mathbf{r}) = \left(\frac{\delta \varepsilon_i}{\delta v(\mathbf{r})}\right)_N \tag{18}$$

Recently a straightforward scheme to evaluate these kind of derivatives was presented by the present authors in collaboration with P. W. Ayers.[27,48,49] We slightly improved the code for this study to include second-order effects and to take advantage of the molecular symmetry (vide infra). Details on the initial approach, its validation, and numerical results can be found in the literature.[27,48,49]

Consider a functional Taylor series expansion of the orbital energy ε_i as a functional of $v(\mathbf{r})$ up to second order:

$$\varepsilon_i[v(\mathbf{r}) + \Delta v(\mathbf{r})] = \varepsilon_i[v(\mathbf{r})] + \int \left(\frac{\delta \varepsilon_i}{\delta v(\mathbf{r})}\right)_N\Big|_{\Delta v(\mathbf{r})=0} \Delta v(\mathbf{r})\mathrm{d}\mathbf{r} + \frac{1}{2}\iint \left(\frac{\delta^2 \varepsilon_i}{\delta v(\mathbf{r})\delta v(\mathbf{r}')}\right)_N\Big|_{\Delta v(\mathbf{r})=0} \Delta v(\mathbf{r})\Delta v(\mathbf{r}')\mathrm{d}\mathbf{r}\mathrm{d}\mathbf{r}' \quad (19)$$

Choosing the perturbations $\Delta v(\mathbf{r})$ in eq 19 of the external potential as $u_j(\mathbf{r})$ and $-u_j(\mathbf{r})$ and subtracting the corresponding expressions gives

$$\frac{1}{2}(\varepsilon_i[v(\mathbf{r}) + u_j(\mathbf{r})] - \varepsilon_i[v(\mathbf{r}) - u_j(\mathbf{r})]) = \int f_i^-(\mathbf{r})u_j(\mathbf{r})\mathrm{d}\mathbf{r} \quad (20)$$

The Fukui function $f_i^-(\mathbf{r})$ can now be found by expanding it in a basis set $\{\beta_k(\mathbf{r})\}_{k=1}^M$,

$$f_i^-(\mathbf{r}) = \sum_{k=1}^{M} c_k^i \beta_k(\mathbf{r}) \quad (21)$$

and solving the following set of linear equations for the unknown expansion coefficients c_k^i:

$$\frac{1}{2}(\varepsilon_i[v(\mathbf{r}) + u_j(\mathbf{r})] - \varepsilon_i[v(\mathbf{r}) - u_j(\mathbf{r})]) = \sum_{k=1}^{M} c_k^i \int \beta_k(\mathbf{r})u_j(\mathbf{r})\mathrm{d}\mathbf{r} \quad (22)$$

where the index j runs over 1 to P. As P is generally chosen to be much larger than M in order to provide an adequate description of the functional derivative, the set of eq 22 can be solved by a linear least-squares procedure.

The practical application of this approach requires a set of P perturbations $\{u_j(\mathbf{r})\}_{j=1}^P$ and their negative counterparts to be defined so as to calculate the left-hand side of eq 22. We will perturb the external potential by placing point charges in the molecular environment. For every positive point charge q_j the orbital energy $\varepsilon_i[v(\mathbf{r}) + u_j(\mathbf{r})]$ can be calculated by means of a single-point energy calculation as is the case for its negative counterpart $-q_j$ for which the corresponding orbital energy $\varepsilon_i[v(\mathbf{r}) - u_j(\mathbf{r})]$ is found. The integrals on the right-hand side of eq 22 are readily obtained as the perturbations $\{u_j(\mathbf{r})\}_{j=1}^P$ and the basis functions $\{\beta_k(\mathbf{r})\}_{k=1}^M$, for which s- and p-type Gaussians will be used, are known. Further details on the kind of basis functions and the characteristics of the point charges are given in paragraph 4.2.

We conclude this methodological section with a few notes on the weighting factors w_i in eq 17. As the central surface oxygen atom $O_{central}$ in our clusters (see Figure 1a) constitutes the reactive site of interest, the weighting factors should be proportional to the contribution of this atom to the various MOs entering eq 17. We will use a Mulliken population analysis[50] type of argument to give a rough estimate of this contribution. Since every molecular orbital $\psi_i(\mathbf{r})$ is expanded in a basis of atomic orbitals (AOs) $\phi_k(\mathbf{r})$, taken real for the sake of simplicity,

$$\psi_i(\mathbf{r}) = \sum_{k}^{\mathrm{AO}} d_k^i \phi_k(\mathbf{r}) \quad (23)$$

the share of $O_{central}$ in its integrated probability distribution can be estimated as $\sum_k^{O_{central}} \sum_l d_k^i d_l^i S_{kl}$, where S_{kl} is the overlap integral of two atomic orbitals k and l. A practical expression for w_i is obtained after normalization:

$$w_i = \left(\sum_k^{O_{central}} \sum_l d_k^i d_l^i s_{kl}\right) \Big/ \left(\sum_j \sum_k^{O_{central}} \sum_l d_i^i d_l^i s_{kl}\right) \quad (24)$$

where the summation over j includes all the MOs taken into account in eq 17.

4.2. Surface Reactivity Trend. The actual calculation of the functional derivatives requires the choice of a number of parameters. We refer to our previous studies[27,48,49] for a detailed description of the parameter optimization and immediately proceed to give the technical specifications used in the present study. The perturbations $\{\pm u_j(\mathbf{r})\}_{j=1}^P$ of the external potential are modeled as positive and negative point charges which are placed on a cubic grid within a region characterized by three scaled molecular van der Waals surfaces. Perturbations located between the surfaces scaled by the factors 0.05 and 0.75 are assigned charge values of ± 0.02 au, and those situated between the 0.75 and 2.50 scaled surfaces have charges of ± 0.05 au. The perturbations lying deeply in the molecular electron density only bear a small amount of charge so that the second-order approximation to the functional Taylor series expansion (eq 19) is justified.

Given the C_{4v} symmetry of the clusters under consideration, not the entire system but only one-eighth of it should be sampled by perturbations. Through the use of the molecular symmetry, these data can be multiplied throughout space to provide the necessary information for the calculation of the functional derivatives of the whole system (eq 22). We worked with a number of about 1500 perturbations, which totals a number of 12 000 perturbations after symmetry-based multiplication. The corresponding data set is largely sufficient to ensure well-converged results.

The basis set in which the functional derivatives are expanded (eq 21) is made up of the uncontracted s- and p-type functions of the Ahlrichs Coulomb fitting auxiliary basis set.[51] This density-based set is typically used for the acceleration of the evaluation of the Coulomb integrals in DFT calculations and has proven to be very successful in the representation of Fukui functions. The single-point calculations are carried out at the same level of theory as explained in section 3.2, except for the exchange-correlation functional that is replaced by the PBE approximation.[52]

Figures 1c and 1d give three-dimensional isosurface plots of the standard Fukui function $f^-(\mathbf{r})$ and the MO-averaged

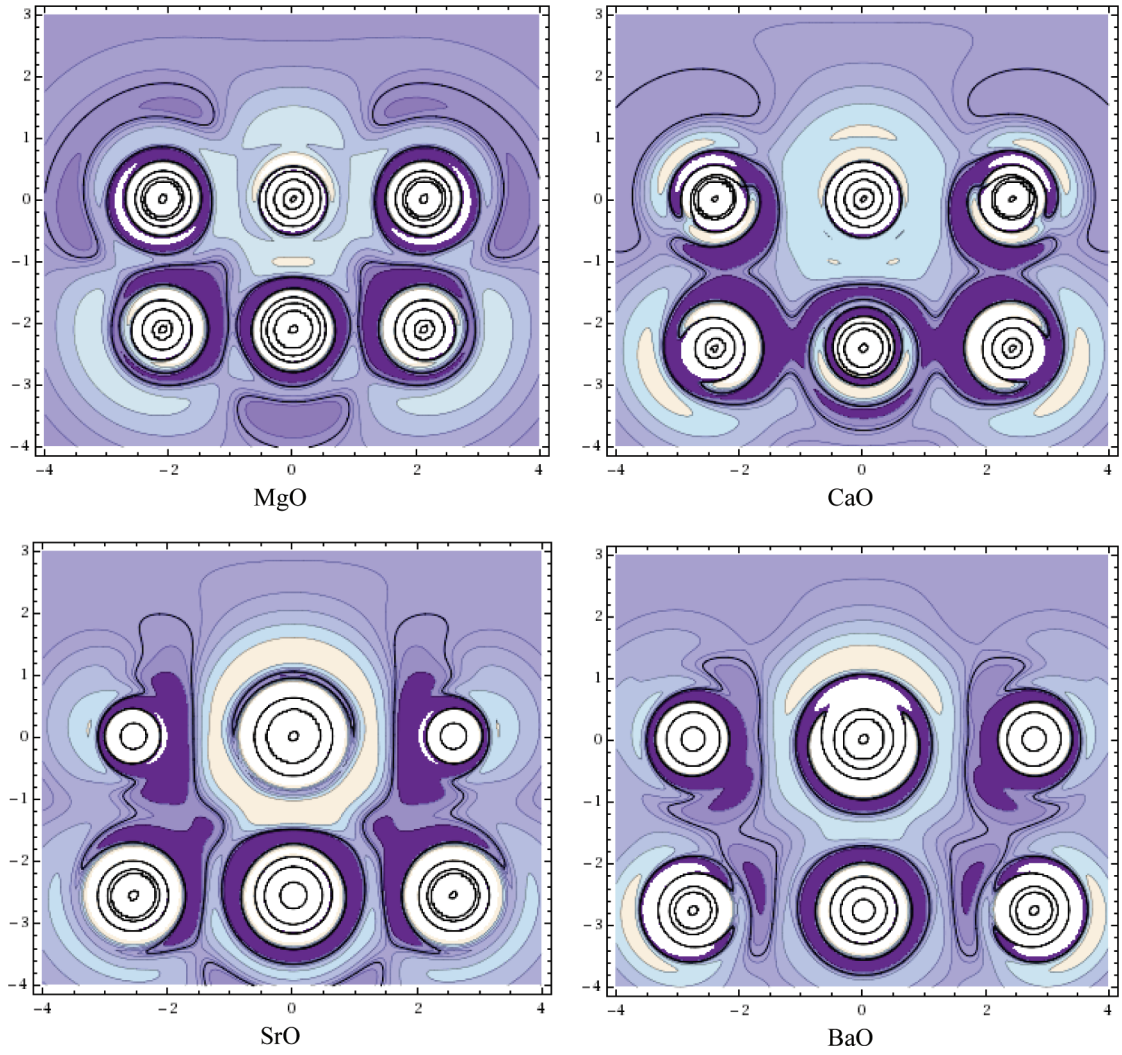

Figure 3. Contour plots of the MO-averaged Fukui function from below $\tilde{f}^{-}(\mathbf{r})$ for the Me_9O_9 clusters (with Me = Mg, Ca, Sr, or Ba), perpendicular to the clusters' surface. The contour values n_i (in au) are obtained as $n_i = 2 \times 10^{-5}\, i^3 - 3 \times 10^{-5}\, i^2 + 10^{-4}\, i$, with $i \in \{-2, -1, ..., 5\}$. The zero-contour is printed in bold and lighter regions are associated with higher values. The central surface oxygen atom lies at the (0 Å, 0 Å) coordinate.

function $\tilde{f}^{-}(\mathbf{r})$ for the Sr_9O_9 cluster. The standard Fukui function is predominantly located on the oxygens of the cluster edges and consequently does not provide a valuable description of the central oxygen, which is, as stated above, the best described quantum atom and should be used for the construction of an intermolecular reactivity scale. This erroneous behavior is directly linked to the electron distribution of the HOMO, which is not very pronounced at this central atom and is thus not the orbital that should be used to discuss the chemical reactivity. The introduction of the molecular orbitals made up of the O-2p atomic orbitals, as suggested in paragraph 3.2, in the calculation of the MO-averaged Fukui function $\tilde{f}^{-}(\mathbf{r})$ dramatically improves the results, however. Figure 1d gives the corresponding plot, which clearly shows how the central oxygen atom now governs the reactivity description of the cluster. As an analysis of the other systems (Mg_9O_9, Ca_9O_9, and Ba_9O_9) leads to analogous conclusions, the intercluster reactivity trend can now be constructed.

Figure 3 provides contour plots of the MO-averaged Fukui functions for the various Me_9O_9 systems. They are given in a plane perpendicular to the clusters' surface. Analysis of the contour lines at the central surface oxygen atom reveals that the values of the MO-averaged Fukui function increase as one goes down the periodic table, but somewhat stagnate between SrO and BaO, where no obvious difference can be noticed. This kind of result is of particular importance in the prediction and interpretation of a system's inherent reactivity toward electrophilic attacks, as the (MO-averaged) Fukui function is a measure of the change in electronic energy of the system under study when it undergoes a simultaneous change in external potential and in its number of electrons. A detailed discussion on this subject can be found in ref 53. The results can thus prove advantageous in the description of adsorption characteristics, catalytic activity, or reaction mechanisms. An increased catalytic activity trend from MgO to BaO has for example been found on the basis of experimental data for the destructive adsorption of carbon tetrachloride, a soft reagent which typically requests a soft reactivity index as the Fukui function in a theoretical analysis.[15]

The trend of increasing reactivity following the trends of increasing cation size and decreasing ionicity of the systems is extensively discussed in a previous study by some of the

present authors.[20] That study focused on the investigation of the local softness $s(\mathbf{r})$ of the alkaline earth oxide series through a periodic boundary conditions (PBC) approach and the use of the local density of states $g(r,E)$:[26,54]

$$s(\mathbf{r}) = \lim_{\delta\mu\to 0} \frac{1}{\delta\mu} \int_{\mu-\delta\mu}^{\mu} g(\mathbf{r}, E)\mathrm{d}E \qquad (25)$$

The fact that our results are also in agreement with their theoretical observations proves that our simple cluster model serves as a valuable and straightforward alternative to the infinite system approach. It is interesting to stress that our MO-averaged Fukui function concept occupies an intermediate place between the standard Fukui functions and the density of states-based descriptors. The former only use one frontier orbital in the description of a molecule's reactivity, whereas the latter utilize a band of orbitals to account for the reactivity of infinite systems. The use of an MO-averaged Fukui function $\tilde{f}(\mathbf{r})$ will typically prove to be beneficial in the intermediate situations where the valence orbitals are closely enough spaced to play an important role in the chemistry and yet do not form a continuous band.

5. Conclusion

Central in this paper is the reliable computation of a DFT-based reactivity index, the Fukui function, for cluster models of solid-state compounds. In the first part, we introduced the MO-averaged Fukui function concept $\tilde{f}^{-}(\mathbf{r})$. Its necessity comes from the observation that standard DFT reactivity descriptors assign a prominent role to the HOMO and the LUMO, but that these orbitals do not always satisfactorily represent the reactive site of interest. $\tilde{f}^{-}(\mathbf{r})$ bypasses this shortcoming by systematically placing some other, well-chosen MOs on the same footing.

The calculation of this new descriptor has been applied to the study of the alkaline earth oxide series. In order to avoid the PBC approach, we performed cluster-based calculations. It has been shown that a medium-sized quantum cluster embedded in an array of point charges is a sound model for the representation of this kind of systems, provided that the embedding charges are adequately optimized. The recovery of the experimental lattice parameter upon geometry optimization of the clusters has proven to be a straightforward and reliable way to obtain the required charges.

The final target of this contribution was the calculation of functional derivatives with respect to the external potential, for which an in-house method has been applied. Together, these three topics offer a valuable alternative to the density of states-based DFT concepts resulting from infinite system calculations. It has indeed been shown that for a series of alkaline earth oxides the results obtained in our work are completely in line with the PBC calculations invoking the local density of states to compute the Fukui function.

Acknowledgment. P.G. and F.D.P. acknowledge the Vrije Universiteit Brussel (VUB) and the Research Foundation - Flanders (FWO) for continuous support to their research group. N.S. acknowledges the FWO for a position as research assistant.

References

(1) Parr, R. G.; Yang, W. *Density Functional Theory of Atoms and Molecules*; Oxford University Press: New York, 1989; pp 1−333.

(2) Chermette, H. *J. Comput. Chem.* **1999**, *20*, 129–154.

(3) Geerlings, P.; De Proft, F.; Langenaeker, W. *Chem. Rev.* **2003**, *103*, 1793–1873, references therein.

(4) Geerlings, P.; De Proft, F. *Phys. Chem. Chem. Phys.* **2008**, *10*, 3028–3042.

(5) Parr, R. G.; Donnelly, R. A.; Levy, M.; Palke, W. E. *J. Chem. Phys.* **1978**, *68*, 3801–3807.

(6) Parr, R. G.; Pearson, R. G. *J. Am. Chem. Soc.* **1983**, *105*, 7512–7516.

(7) Parr, R. G.; Yang, W. J. *J. Am. Chem. Soc.* **1984**, *106*, 4049–4050.

(8) Ayers, P. W.; Levy, M. *Theor. Chem. Acc.* **2000**, *103*, 353–360.

(9) Kohn, W.; Sham, L. J. *Phys. Rev. A* **1965**, *140*, 1133–1138.

(10) Hohenberg, P.; Kohn, W. *Phys. Rev. B* **1964**, *136*, 864–871.

(11) Yang, W.; Parr, R. G.; Pucci, R. *J. Chem. Phys.* **1984**, *81*, 2862–2863.

(12) Senet, P. *J. Chem. Phys.* **1997**, *107*, 2516–2524.

(13) Ayers, P. W. *Theor. Chem. Acc.* **2001**, *106*, 271–279.

(14) Soick, M.; Buyevskaya, O.; Höhenberger, M.; Wolf, B. *Catal. Today* **1996**, *32*, 163–169.

(15) Weckhuysen, B. M.; Mestl, G.; Rosyneck, M. P.; Krawitz, T. R.; Haw, J. F.; Lunsford, J. H. *J. Phys. Chem. B* **1998**, *102*, 3773–3778.

(16) Grönbeck, H.; Broqvist, P.; Panas, I. *Surf. Sci.* **2006**, *600*, 403–408.

(17) Grönbeck, H.; Broqvist, P. *J. Chem. Phys.* **2003**, *119*, 3896–3904.

(18) Zecchina, A.; Scarano, D.; Bordiga, S.; Spoto, G.; Lamberti, C. *Adv. Catal.* **2001**, *46*, 265–397.

(19) Ono, Y.; Baba, T. *Catal. Today* **1997**, *38*, 321–337.

(20) Cárdenas, C.; De Proft, F.; Chamorro, E.; Fuentealba, P.; Geerlings, P. *J. Chem. Phys.* **2008**, *128*, 034708.

(21) Perdew, J. P.; Parr, R. G.; Levy, M.; Balduz, J. L. *Phys. Rev. Lett.* **1982**, *49*, 1691–1694.

(22) Zhang, Y.; Yang, W. *Theor. Chem. Acc.* **2000**, *103*, 346–348.

(23) Ayers, P. W. *J. Math. Chem.* **2008**, *43*, 285–303.

(24) Janak, J. F. *Phys. Rev. B* **1978**, *18*, 7165–7168.

(25) Chan, G. K.-L. *J. Chem. Phys.* **1999**, *110*, 4710–4723.

(26) Cohen, M. H.; Ganduglia-Pirovano, M. V. *J. Chem. Phys.* **1994**, *101*, 8988–8997.

(27) Fievez, T.; Sablon, N.; De Proft, F.; Ayers, P. W.; Geerlings, P. *J. Chem. Theory Comput.* **2008**, *4*, 1065–1072.

(28) Sauer, J. *Chem. Rev.* **1989**, *89*, 199–255.

(29) Kadossov, E. B.; Gaskell, K. J.; Langell, M. A. *J. Comput. Chem.* **2007**, *28*, 1240–1251.

(30) Stefanovich, E. V.; Truong, T. N. *J. Chem. Phys.* **1996**, *104*, 2946–2955.

(31) Xu, X.; Nakatsuji, H.; Lu, X.; Ehara, M.; Cai, Y.; Wang, N. Q.; Zhang, Q. E. *Theor. Chem. Acc.* **1999**, *102*, 170–179.

(32) Lü, X.; Xu, X.; Wang, N.; Zhang, Q.; Ehara, M.; Nakatsuji, H. *Chem. Phys. Lett.* **1998**, *291*, 445–452.

(33) Xu, X.; Lü, X.; Wang, N.; Zhang, Q. *Chem. Phys. Lett.* **1995**, *235*, 541–547.

(34) (a) Field, M. J.; Bash, P. A.; Karplus, M. *J. Comput. Chem.* **1990**, *11*, 700–733. (b) Masera, F.; Morokuma, K. *J. Comput. Chem.* **1995**, *16*, 1170–1179.

(35) (a) Vail, J. M. *J. Phys. Chem. Solids* **1990**, *51*, 589–607. (b) Yudanov, I. V.; Nasluzov, V. A.; Neyman, K. M.; Rösch, N. *Int. J. Quantum Chem.* **1997**, *65*, 975–986.

(36) Stefanovich, E. V.; Truong, T. N. *J. Phys. Chem. B* **1998**, *102*, 3018–3022.

(37) Sousa, C.; Casanovas, J.; Rubio, J.; Illas, F. *J. Comput. Chem.* **1993**, *14*, 680–684.

(38) Huang, Z. H.; Guo, H. *Surf. Sci.* **1993**, *286*, 182–189.

(39) Rittner, F.; Fink, R.; Boddenberg, B.; Staemmler, V. *Phys. Rev. B* **1999**, *57*, 4160–4171.

(40) Derenzo, S. E.; Klintenberg, M. K.; Weber, M. J. *J. Chem. Phys.* **2000**, *112*, 2074–2081.

(41) Batista, E. R.; Friesner, R. A. *J. Phys. Chem. B* **2002**, *106*, 8136–8141.

(42) Xu, X.; Nakatsuji, H.; Ehara, M.; Lü, X.; Wang, N. Q.; Zhang, Q. E. *Chem. Phys. Lett.* **1998**, *292*, 282–288.

(43) (a) Cerjan, C. J.; Miller, W. H. *J. Chem. Phys.* **1981**, *75*, 2800–2806. (b) Simons, S.; Jorgensen, P.; Taylor, H.; Ozment, J. *J. Phys. Chem.* **1983**, *87*, 2745–2753. (c) Bannerjee, A.; Adams, N.; Simons, J.; Shepard, R. *J. Phys. Chem.* **1985**, *89*, 52–57.

(44) (a) Lee, C.; Yang, W.; Parr, R. G. *Phys. Rev. B* **1988**, *37*, 785–789. (b) Becke, A. D. *J. Chem. Phys.* **1993**, *98*, 5648–5652. (c) Stevens, P. J.; Delvin, F. J.; Chablaoski, C. F.; Frisch, M. J. *J. Phys. Chem.* **1994**, *98*, 11623–11627.

(45) Hehre, W. J.; Radom, L.; Schleyer, P. v. R.; Pople, J. A. *Ab Initio Molecular Orbital Theory*; Wiley: New York, 1986; Chapter 4; pp 65−88.

(46) Kaupp, M.; Schleyer, P. v. R.; Stoll, H.; Preuss, H. *J. Chem. Phys.* **1991**, *94*, 1360–1366.

(47) Frisch, M. J.; Trucks, G. W.; Schlegel, H. B.; Scuseria, G. E.; Robb, M. A.; Cheeseman, J. R.; Montgomery,Jr. J. A.; Vreven, T.; Kudin, K. N.; Burant, J. C.; Millam, J. M.; Iyengar, S. S.; Tomasi, J.; Barone, V.; Mennucci, B.; Cossi, M.; Scalmani, G.; Rega, N.; Petersson, G. A.; Nakatsuji, H.; Hada, M.; Ehara, M.; Toyota, K.; Fukuda, R.; Hasegawa, J.; Ishida, M.; Nakajima, T.; Honda, Y.; Kitao, O.; Nakai, H.; Klene, M.; Li, X.; Kno J. E.; Hratchian, H. P.; Cross, J. B.; Bakken, V.; Adamo, C.; Jaramillo, J.; Gomperts, R.; Stratmann, R. E.; Yazyev, O.; Austin, A. J.; Cammi, R.; Pomelli, C.; Ochterski, J. W.; Ayala, P. Y.; Morokuma, K.; Voth, G. A.; Salvador, P.; Dannenberg, J. J.; Zakrzewski, V. G.; Dapprich, S.; Daniels, A. D.; Strain, M. C.; Farkas, O.; Malick, D. K.; Rabuck, A. D.; Raghavachari, K.; Foresman, J. B.; Ortiz, J. V.; Cui, Q.; Baboul, A. G.; Clifford, S.; Cioslowski, J.; Stefanov, B. B.; Liu, G.; Liashenko, A.; Piskorz, P.; Komaromi, I.; Martin, R. L.; Fox, D. J.; Keith, T.; Al-Laham, M. A.; Peng, C. Y.; Nanayakkara, A.; Challacombe, M.; Gill, P. M. W.; Johnson, B.; Chen, W.; Wong, M. W.; Gonzalez, C.; Pople, J. A. Gaussian 03, Revision D.01, Gaussian, Inc., Wallingford, CT, 2005.

(48) Ayers, P. W.; De Proft, F.; Borgoo, A.; Geerlings, P. *J. Chem. Phys.* **2007**, *126*, 224107.

(49) Sablon, N.; Ayers, P. W.; De Proft, F.; Geerlings, P. *J. Chem. Phys.* **2007**, *126*, 224108.

(50) Mulliken, R. S. *J. Chem. Phys.* **1934**, *2*, 782–793.

(51) (a) Eichkorn, K.; Treutler, O.; Öhm, H.; Häser, M.; Ahlrichs, R. *Chem. Phys. Lett.* **1995**, *240*, 283–289. (b) Eichkorn, K.; Weigend, F.; Treutler, O.; Ahlrichs, R. *Theor. Chem. Acc.* **1997**, *97*, 119–124.

(52) Perdew, J. P.; Burke, K.; Ernzerhof, M. *Phys. Rev. Lett.* **1996**, *77*, 3865–3868.

(53) Ayers, P. W.; Anderson, J. S. M.; Bartolotti, L. J. *Int. J. Quantum Chem.* **2005**, *101*, 520–534.

(54) (a) Brommer, K. D.; Galván, M.; Dal Pino, A.; Joannopoulos, J. D. *Surf. Sci.* **1994**, *314*, 57–70. (b) Nguyen, L. T.; De Proft, F.; Amat, M. C.; Van Lier, G.; Fowler, P. W.; Geerlings, P. *J. Phys. Chem. A* **2003**, *107*, 6837–6842.

CT9000312